Published in
Applied Physics B : Lasers and Optics 96, issue 4, 863-874, 2009
which should be used for any reference to this work

Self-mixing interference effects in tunable diode laser absorption spectroscopy

D. Masiyano · J. Hodgkinson · S. Schilt · R.P. Tatam

Abstract We report the effects of self-mixing interference on gas detection using tunable diode laser spectroscopy. For very weak feedback, the laser diode output intensity gains a sinusoidal modulation analogous to that caused by low finesse etalons in the optical path. Our experiments show that self-mixing interference can arise from both specular reflections (e.g. cell windows) and diffuse reflections (e.g. Spectralon™ and retroreflective tape), potentially in a wider range of circumstances than etalon-induced interference. The form and magnitude of the modulation is shown to agree with theory. We have quantified the effect of these spurious signals on methane detection using wavelength modulation spectroscopy and discuss the implications for real gas detectors.

D. Masiyano · J. Hodgkinson (✉) · R.P. Tatam
Engineering Photonics Group, School of Engineering, Cranfield University, Bedfordshire MK43 0AL, UK
e-mail: j.hodgkinson@cranfield.ac.uk

Present address:
D. Masiyano
Alps Electric (UK) Ltd, Garamonde Drive, Wymbush, Milton Keynes MK8 8LW, UK

S. Schilt
IR Microsystems, Rue Daniel Colladon, PSE-C, 1015 Lausanne, Switzerland

Present address:
S. Schilt
Laboratoire Temps-Fréquence (LTF), Université de Neuchâtel, Avenue de Bellevaux 51, 2009 Neuchâtel, Switzerland

1 Introduction

Tunable diode laser spectroscopy (TDLS) is a high-resolution spectroscopic technique in which the emission from a laser diode is scanned or modulated across the wavelength corresponding to a single absorption line of a target gas [1]. Gas absorption linewidths are narrow (full width at half maximum of ∼5 GHz at atmospheric pressure), and therefore to resolve the gas line requires the use of lasers with narrower emission linewidths; tens of MHz is typical. One consequence is the long coherence length of the laser emission (typically tens of metres), with the potential for optical interference arising from etalons lying on the optic axis. For the "wrong" length of etalon, the resulting interference fringes appear as unwanted spectral features that can be indistinguishable from the absorption line of the measurand.

The gas sample cells themselves have been considered to be frequent culprits [2], because typical lengths of the order of 30 mm give rise to etalons with a free spectral range of the order of 5 GHz. Despite the use of wedged windows and antireflection coated optics, small Fresnel reflections often persist in the optical path [1] or develop after a period of time in the field [3]. Over time, fluctuations in temperature and/or vibrations of the etalon cause the interference fringes to shift in wavelength such that they cannot be removed by subtraction of a zero baseline. In practical systems, the resulting uncertainty is often considered to be the limiting factor in gas detection performance at low concentrations. Various post-detection filtering schemes exist to remove the unwanted spectral features [1], but in the main these rely on those features having a width that notably differs from that of the absorption line.

The phenomenon of laser diode self-mixing is well known as a means of measuring the deflection of surfaces in a direction normal to the optic axis [4]. Figure 1 shows a

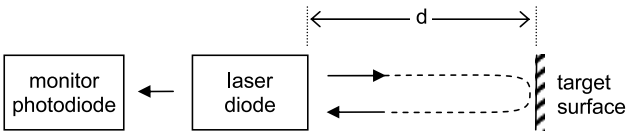

Fig. 1 Typical schematic configuration for measurement of deflection using laser diode self-mixing. After Guiliani et al. [4]

simplified example. The light from a laser diode leaves the front facet and, sometimes after passing through a collimating lens, is directed towards the target surface. Reflections or scattered light are directed back towards the laser diode front facet, often but not always with the aid of the collimating lens, which may be enlarged to collect more of the reflected light. Feedback effects within the laser diode create an output intensity modulation that is periodic in the optical phase difference induced by surface displacement or wavelength changes. This modulation can be monitored on the output from the rear facet, using the monitor photodiode which is often found in the laser diode package. A typical set-up involves the use of a single-mode Fabry–Perot laser diode, but self-mixing interference has been demonstrated using both distributed feedback (DFB) laser diodes [5] and vertical-cavity surface-emitting lasers (VCSELs) [6]. Self-mixing interference has been observed using mirrors as targets and from rough surfaces, where the returned light takes the form of a speckle field [7].

We report observations of self-mixing induced spectral features in the absorption spectra measured for TDLS-based gas detection. These features are almost identical in appearance to interference fringes and can create equally problematic measurement uncertainties that limit detector performance. To our knowledge, self-mixing interference or feedback interference has not been previously reported in TDLS, though it may have been widely observed. The effect is difficult to distinguish from etalon-induced interference fringes, and as we show, it can arise in a greater range of circumstances than is the case for etalons. In particular, this phenomenon is particularly relevant to the use of diffusely reflective surfaces within gas cells.

2 Theory

2.1 Gas detection

Methane has a well-known $2\nu_3$ absorption band in the near infrared region of the spectrum, centred around 1.66-μm, shown in Fig. 2. Our studies concentrate on the R4 quadruplet line at 1.651 μm.

For monochromatic radiation, the level of light transmitted through a gas cell is given by the Beer–Lambert law,

$$I = I_0 \exp(-\alpha z) \tag{1}$$

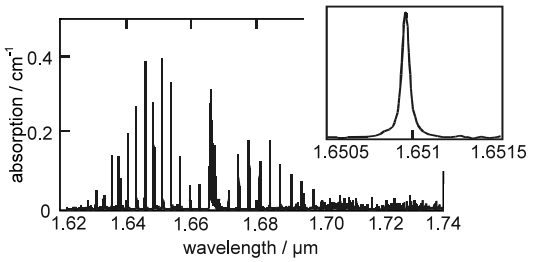

Fig. 2 Absorption spectrum for 100% methane in the near infra-red, calculated using data from the HITRAN database [8]

where I_0 is the light power transmitted in the absence of light absorption, α is the absorption coefficient of the measurand in cm^{-1} (equal to the specific absorptivity of the gas ε multiplied by the gas concentration) and z is the pathlength (here in cm). The gas absorptivity is often expressed in units of cm^{-1} per unit partial pressure of gas; at 1651-nm and at atmospheric pressure, methane has a value of ε at the line centre of 0.38 cm^{-1} atm^{-1} [8]. At low values of αz, (1) approximates to the following linear relationship:

$$I \approx I_0(1 - \alpha z) \tag{2}$$

2.2 Interference from low finesse etalons

Low-finesse Fabry–Perot etalons within the optical path give rise to an intensity modulation that takes the form [9]

$$I = I_0\{1 + K\cos\delta\} \tag{3}$$

where I_0 is the incident intensity, λ is the wavelength, K is a constant whose value lies between zero and one and δ is the optical phase of the cavity of length d, with $\delta = 4\pi d/\lambda$ for a cavity round trip (see Fig. 3). The value of K is proportional to $\sqrt{r_1 r_2}$, where r_1 and r_2 are the reflectivities of the two surfaces forming the etalon. If the reflectivities of the two surfaces are equal ($r_1 = r_2 = r$), as might be expected in the case of windows, K varies in proportion to r.

The light reflected from the cavity is also modulated, such that it is out of phase by 180° in δ with respect to the transmitted intensity. The light modulation occurs outside the laser cavity, and the laser itself is unaffected. The total level of light emitted from the diode (transmitted + reflected) is therefore constant, as is the voltage across the laser diode at a given drive current.

2.3 Interferometric speckle

If coherent light is incident on an optically rough surface, the returned light can take the form of a speckle field. In speckle interferometry, the speckle is deliberately mixed with a reference beam [10]. The principle applies to an in-line configuration relevant to the geometry of a gas absorption cell,

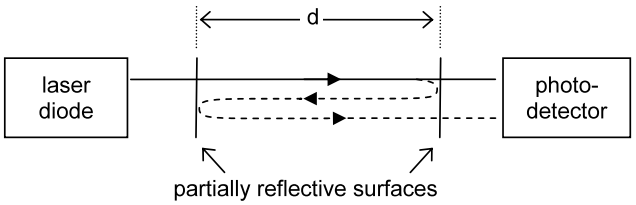

Fig. 3 A low-finesse etalon in the optical path of a detection system; the partially reflective surfaces are often the windows of the gas sample cell

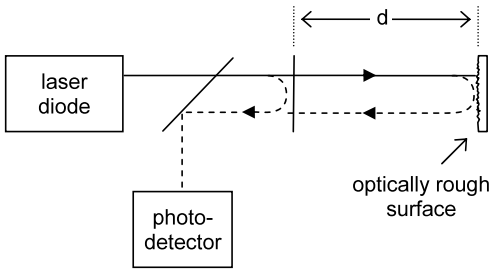

Fig. 4 Observation of interferometric speckle in an in-line configuration

as shown in Fig. 4, for which the reference beam is created by the partial reflection from an optical surface such as one side of a cell window, and a speckle pattern is produced by scattering from a diffuse surface after a further distance d.

In speckle interferometry, the speckle field is imaged to provide spatial information about the target surface, but here the speckles are simply integrated over the surface of a single detector. Interference features in the speckle image are termed correlation fringes and represent an intensity modulation of the randomised speckle field. We have previously demonstrated such an intensity modulation arising from a gas cell that uses a diffusely reflective surface [11]. Sirohi has shown that the intensity modulation at the detector takes the form [12]

$$I = I_0(1 + A\cos\delta) \tag{4}$$

The constant A is proportional to $\sqrt{I_1 I_2}$, where I_1 and I_2 are the intensities of the reference beam and speckle field, respectively. For a gas cell incorporating a window (giving the reference beam) and a diffusely reflective surface (giving the speckle field), the fringe amplitude is proportional to $\sqrt{r_1 r_2}$, where r_1 and r_2 are the surface reflectivities.

2.4 Self-mixing interference

Giuliani et al. [4] have characterised the form of self-mixing interference for a general case of single-mode Fabry–Perot laser diodes, according to the level of feedback reaching the laser. The conditions described in our experimental section correspond to their "very weak feedback" regime, in which the lasers maintain single-mode behaviour. The laser output intensity takes the form

$$I = I_0(1 + M\cos\delta) \tag{5}$$

where I_0 is the output power from the diode in the absence of feedback, I is the modulated power output in the presence of feedback and M is described as a modulation index (not to be confused with the modulation index m used in TDLS, which describes the ratio of the sinusoidal source modulation to the gas linewidth). M is a function of the so-called feedback parameter C (dependent on the characteristics of the laser) and, for very weak feedback, proportional to $\sqrt{r}$ where r is the proportion of light reflected back into the laser diode.

This form of intensity modulation that is observed at the photodetector is therefore indistinguishable from (3), but the effects differ from those of etalon interference in two ways. Firstly, the result is a modulation of the output intensity of the laser diode rather than of the intensity of light transmitted or reflected from the interfering cavity. The output from the rear facet is also modulated with a 180° phase change in δ, compared to the front facet. Secondly, while the laser drive current is ramped, a modulation can also be observed on the voltage across the diode [4]. The laser itself is thus affected in the case of self-mixing, forming part of the interfering cavity.

For a perfect Lambertian diffuse reflector, the level of returned light I into a small solid angle $\delta\Omega$ is given by

$$r = \frac{\delta I}{I_0} = \frac{3}{4\pi} F(1 + \cos 2\theta)\delta\Omega \tag{6}$$

F is the fraction of light backscattered in total by the diffuser (= 0.99 for Spectralon and similar materials, as used in our experiments), and θ is the angle that the collection axis makes to the normal to the surface.

2.5 Effect of wavelength modulation spectroscopy

Wavelength modulation spectroscopy (WMS) is a well-known technique used to detect small absorption signals such as produced by low-concentration gas absorption lines [1]. In WMS, a small sinusoidal modulation at a frequency f (several kHz) is applied to the laser injection current to dither the wavelength emitted by the laser diode, with an amplitude λ_m set approximately equal to the full width at half maximum of the absorption line [1]. The $2f$ component of the output is measured using a lock-in amplifier. It reaches a maximum at the absorption line centre, and its magnitude is proportional to the depth of the absorption at low αz. If the laser centre wavelength is slowly swept across the absorption line (typically at mHz scan rates), the $2f$ signal appears as a second derivative of the absorption feature.

The technique confers greater sensitivity of the measurement to curved spectral features, enabling detection of small absorbances in the range 10^{-5}–10^{-6} for a well-designed optical set-up [1].

However, the high sensitivity of WMS to small absorption features makes the technique also very prone to weak interference fringes. For a sinusoidal interference pattern, there will again be a second derivative-like structure in the second harmonic signal, which also takes the form of a sinusoidal modulation. The amplitude of the fringes in the $2f$ signal depends on the amplitude of the intensity modulation in the direct signal as described by (3), (4) or (5), but also on the ratio of the laser wavelength modulation to the free spectral range of the interference fringes $\Delta\lambda$ [13]. For $\lambda_m \ll \Delta\lambda$, the result as we sweep in wavelength is approximately equal to the second derivative of the underlying spectrum. For $\lambda_m > \Delta\lambda$, the amplitude of the $2f$ fringes varies as a sine function of $(\lambda_m/\Delta\lambda)$ multiplied by an envelope function that is proportional to $(\lambda_m/\Delta\lambda)^{-1/2}$ [13].

2.6 Summary

All the above interference effects can create a modulation of the light intensity at a detector, both in the dc and $2f$ components when WMS is applied. For low levels of returned light and a given cavity length d, the resulting fringes take the same sinusoidal form. The effects of interference from low-reflectivity etalons and from diffuse reflections are equivalent. Interference caused by self-mixing in the laser diode cavity can be distinguished from these effects in two ways:

(i) Measuring a modulation of the output from the laser diode itself, which may conveniently be achieved at the rear facet by using a monitor diode.
(ii) Measuring a modulation of the voltage across the diode. This has a poor signal to noise ratio but is more convenient for laser diodes with no rear emission, such as VCSELs.

Self-mixing interference can be caused by both specular and diffuse reflections with equivalent effects for the same levels of returned light and cavity length.

If multiple sources of interference effects combine, the result will be a combination of intensities taking the form of (3), (4) or (5). For cavities of different lengths, the overall form of the modulation can appear as a series of narrow fringes with a broader envelope.

3 Experimental details

We used a straightforward implementation of WMS at $f = 6$ kHz with second harmonic ($2f$) detection at 12 kHz. We applied a simultaneous slow wavelength scan across the spectrum at mHz rates, in the vicinity of a gas absorption line. A variety of different sample cell geometries was used, and these are described in greater detail in the results section. We also used two different types of laser diode, a distributed feedback (DFB) laser and a vertical cavity surface emitting laser (VCSEL). Figure 5 shows a schematic diagram of our laser diode modulation and detection apparatus, in this case configured for measurement of self-mixing modulation of the rear facet emission from the DFB laser diode.

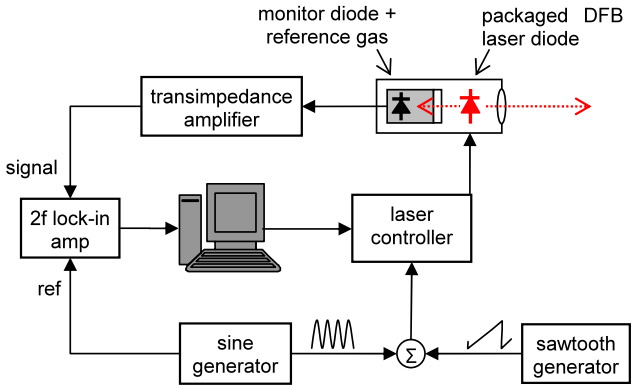

Fig. 5 Schematic experimental configuration for $2f$ wavelength modulation spectroscopy, implemented using the emission from the rear facet of the DFB laser in order to distinguish self-mixing interference from other types of interference

A detector/amplifier (Thorlabs PDA400) was used to detect the forward emission from the laser diode, with a gain of 0 dB (15 kΩ). A lock in amplifier (Stanford Research SR850) was used for $2f$ demodulation, its output voltage (X, in X, Y mode) sampled using a data acquisition card and transferred to a PC for data processing. In the absence of gas, the demodulated $2f$ signal showed a broadly flat baseline with increasing current, as expected. In the presence of methane, at the absorption line centre an increase in the $2f$ signal was observed corresponding to the magnitude of the absorption. Single-mode operation of the laser diodes was confirmed using a confocal Fabry–Perot interferometer (Toptica FPI100, FSR = 1 GHz, Finesse >100). This instrument was also used to determine the current tuning coefficient of our laser diodes over the wide tuning range considered in our experiments, by monitoring the transmission of the interferometer and counting fringes while ramping the laser diode current through its full range.

Test gases were fed to the gas cell from certified cylinders (Scott Specialty Gases), one containing hydrocarbon (HC) free air and the other containing methane in HC free air at a concentration of either 1010 ppm or 2.5 vol%. A bank of mass flow controllers (Teledyne Hastings HFC-302 with THPS-400 controller) was used to control flow rates from the two cylinders, with downstream mixing generating different concentrations in the range 0–2.5 vol%.

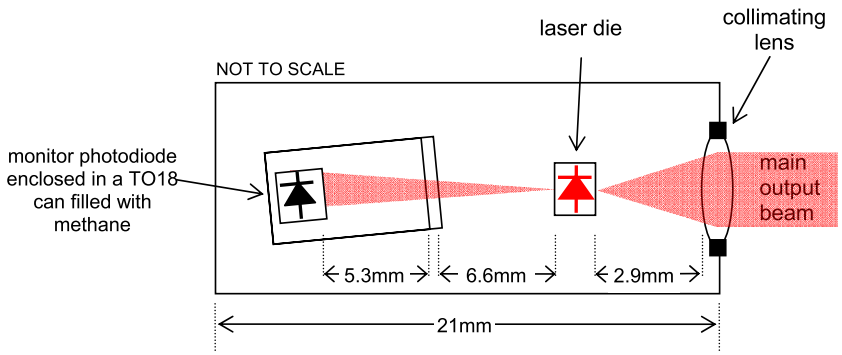

Fig. 6 Optical layout of the DFB laser package, showing key distances between components

3.1 DFB laser diode

Our DFB laser diode package (Semelab Ltd) incorporated a 1650-nm laser (NEL NLK1U5C1CA-TS) collimated with an aspheric lens (Lightpath 350230D) with clear aperture of 4.9 mm. As shown in Fig. 6, behind the rear facet was a gas reference cell, consisting of a Ge photodiode sitting at the bottom of a TO18 can filled with 100% methane. With an internal pathlength of 5.3 mm, this facilitated locking of the laser diode emission to the methane line during gas detection experiments, with the 3f signal component from the Ge photodiode providing our error signal. We also used this monitor photodiode to record self-mixing interference modulation of the laser diode output, in which case the bulk laser temperature was set to provide emission away from a methane absorption line.

The emitted wavelength was scanned across the gas absorption line centre by applying a current ramp through a laser driver (ILX Lightwave, ILX LDC-3722B), the current varying between a minimum of 30 mA and a maximum of 80 mA (corresponding to a frequency range of 33 GHz). For WMS, a sinusoidal dither was also applied at a frequency of 6 kHz and an amplitude of 24 mA (peak-to-peak), giving a peak-to-peak modulation λ_m of 0.3 pm (or 6 GHz expressed as a frequency). Gross wavelength tuning was achieved by controlling the diode temperature using a Peltier element within the package.

3.2 VCSEL diode

A 1686-nm VCSEL (Vertilas, VL-1686-1-SP-A5) was housed in a TO can with angled and antireflection (AR) coated front window. It was driven by a high-precision current controller (Thorlabs LDC 200 VCSEL) and a temperature controller (Thorlabs TED 200). Modulation of the drive current was achieved by supplying the current controller with a 6-kHz sine waveform from a signal generator (Hewlett Packard HP33120A). A ramp signal (2.5 V peak-to-peak) derived from a second signal generator (Stanford Research DS345) was used to scan the laser DC current from 6 mA to 8 mA.

4 Laboratory Results

We investigated the effect of self-mixing feedback on our two laser diodes for a variety of configurations applicable to gas sensing. These included feedback from an AR coated, wedged window, a retroreflector and a diffuse reflector. Most of our experiments were conducted using the DFB laser because it was convenient to monitor self-mixing feedback using the monitor photodiode at the rear facet, but we also confirmed self-mixing feedback in the VCSEL. For these laboratory experiments, we were able to vary the cavity spacing and change the level of feedback reaching the laser. Finally, we made gas measurements in the presence of interference fringes.

4.1 Packaged DFB laser with no external feedback

With no sources of feedback or etalons external to the DFB laser package, we were able to observe a modulation of the laser's output with a fringe period of several GHz. To characterise such large fringes required temperature tuning of the laser while maintaining a constant drive current of 50 mA. The modulation was observed on both the forward and rear emission; Fig. 7 shows signals recorded by the monitor diode (Ge) as well as the signal from the methane reference gas within the can. The second harmonic signal was recorded while the temperature was stepped from 25°C to 53°C. This range spanned two methane absorption lines (R3 and R4 lines of the $2\nu_3$ band), which also allowed precise measurement of the temperature tuning coefficient (-12.8 GHz °C^{-1}).

A small modulation was observed on the laser output, with a periodicity of approximately 1 ± 0.2°C, corresponding to a cavity spacing of 12 ± 2 mm. This modulation was observed on both the rear and forward emissions. The spacing is consistent with self-mixing interference arising within the DFB laser package, such as from the monitor diode (see Fig. 6), and we confirmed that moving the monitor diode caused the interference to change. Although the monitor diode itself was angled to avoid etalon formation, light could still be backscattered from either the photodiode itself, its

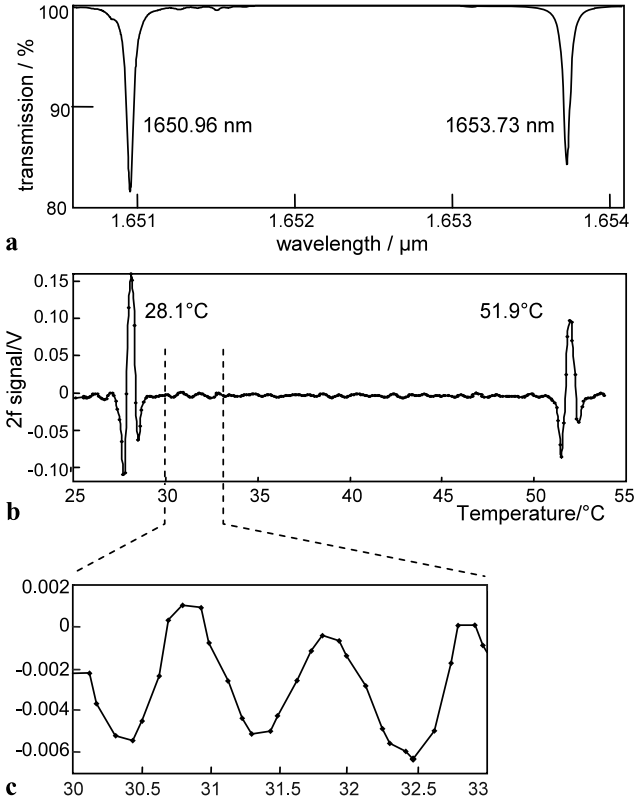

Fig. 7 (**a**) Theoretical methane transmission lines obtained from the Hitran database [8] for a pathlength of 5.3 mm. (**b**) $2f$ signals obtained from the monitor diode while temperature tuning the laser. (**c**) Expansion of (**b**). The fringe spacing was approximately 1 ± 0.2°C, corresponding to a cavity spacing of 12 ± 2 mm

contacts or the header on which it sat. The resulting weak modulation persisted throughout our experiments with this laser, reported below, appearing as a broad envelope for narrower fringes.

4.2 DFB laser with feedback from wedged windows

We conducted an experiment to confirm the behaviour of interference effects due to self-mixing, using the configuration illustrated schematically in Fig. 8. The specular reflection from the front surface of a wedged window was directed back towards the laser diode to induce feedback. This represents a worst-case scenario for gas sensing; typically one would aim to have this reflection aligned away from the optical axis.

A fraction of the main beam was sampled by a beam splitter pellicle beamsplitter (Thorlabs BP245B3, 45:55 split ratio) and directed to a confocal optical spectrum analyser (Toptica FPI100, FSR = 1 GHz, Finesse >100) or detector A (Thorlabs PDA400). A slight tilt was applied to the spectrum analyser/detector A to direct the reflected beam away from the laser. A 6° wedged window was placed in the path of the transmitted beam 154 mm from laser. The optical

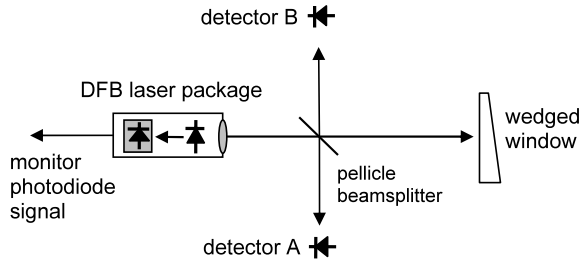

Fig. 8 Schematic diagram of the experimental configuration to measure the effects of feedback from a wedged window

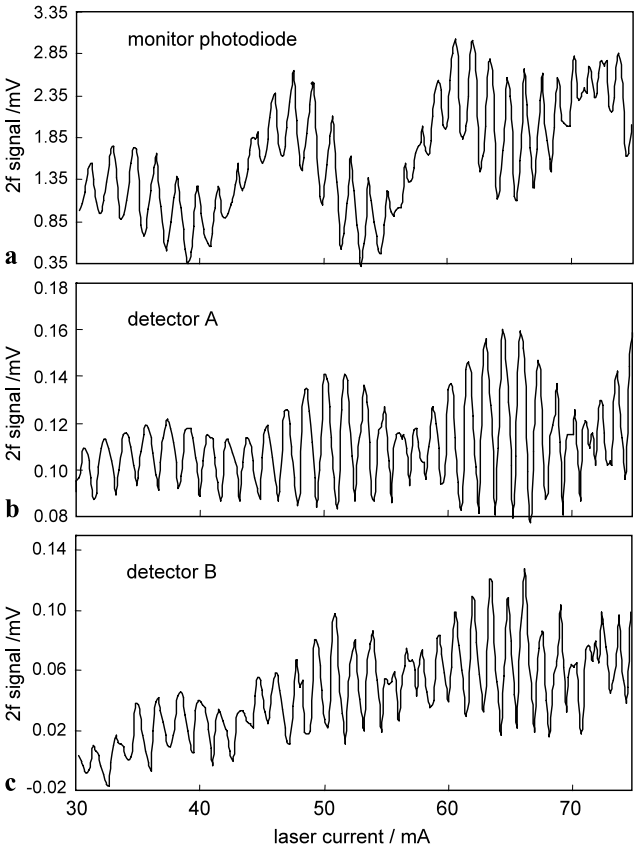

Fig. 9 Interferometric signals caused by feedback from a wedged window placed 154 mm from the laser, obtained at (**a**) the reference photodiode (100 kΩ transimpedance gain), (**b**) detector A (0 dB gain), (**c**) detector B (30 dB gain).The laser temperature was set to 40° (away from the gas line). Note different scales

pathlength of the cavity was estimated to be 154 mm, plus an additional 1.5 mm accounted for by the finite thickness of the collimating lens ($n = 1.586$ at 1550 nm). A fraction of backreflected light from the wedged window was sampled by the beam splitter and directed to detector B (Thorlabs PDA400). After amplification, the signals detected by the reference monitor photodiode, detector A and detector B were then demodulated at $2f$.

The results in Fig. 9 show that high-frequency fringes of the same periodicity were observed at each of the three de-

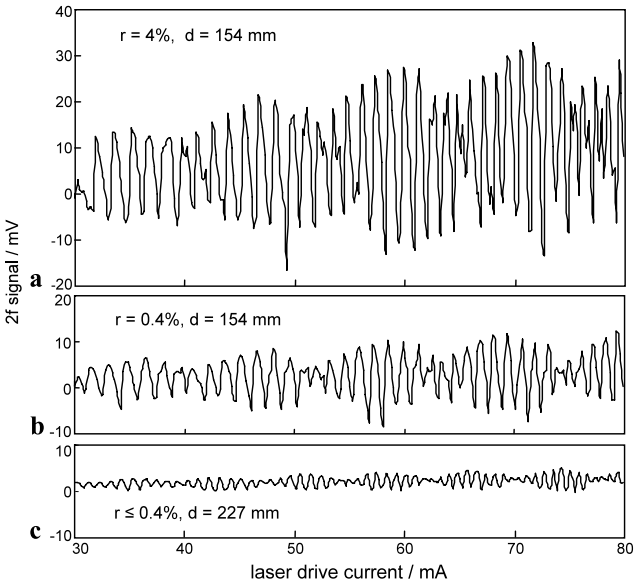

Fig. 10 Self-mixing induced interference fringes observed in the laser diode forward emission for feedback from (**a**) an uncoated 6° wedged window at a distance of 154 mm, (**b**) an AR-coated 6° wedged window at a distance of 154 mm, and (**c**) the latter at a distance of 227 mm

tectors. Using the calibrated tuning coefficient, the cavity length was estimated from these fringes to be 163 ± 8 mm, which compares well with the measured optical pathlength of 155.5 mm.

We conducted a further experiment to quantify self-mixing interference from windows with different reflectivities, in this case comparing a plain wedged window with an AR-coated wedged window (Thorlabs PS812-C). This type of window is routinely used in gas absorption cells to reduce the intensity of specular reflections that might give rise to etalon effects. The AR coating had a specified reflectivity of approximately 0.4% at 1650 nm. The uncoated window (BK7 glass) had a reflectivity estimated to be 4% at 1650 nm. To observe weak feedback with a high signal-to-noise ratio, we recorded the forward emission from the laser diode using detector A in Fig. 9. Where the modulation signal was strong enough to be measurable at the rear facet, it corresponded well with the modulation observed in the forward path.

For self-mixing interference, we expect to see the magnitude of the modulation vary with $\sqrt{r}$, as shown here. At a distance of 154 mm, reducing the surface reflectivity by a factor of approximately 10 has reduced the fringe amplitude by a factor of 2.5, in line with our expectations of a factor of 3.3. Increasing the distance to 227 mm reduced the amplitude by a further factor of approximately 3. However, in the latter case the effect of reducing the cavity FSR is likely to dominate the change in fringe amplitude, as discussed in Sect. 2.5, and we can draw no conclusions from this about the level of self-mixing induced interference.

At a distance of 154 mm, the fringe amplitude obtained with the AR-coated window corresponded to a gas concentration of approximately ± 900 ppm CH_4 in a 100-mm pathlength. Assuming that (5) holds, we would have to reduce the level of feedback to below the level of 1 part in 10^8 to be able to detect methane at the level of 1 ppm.

4.3 DFB laser with feedback from a retroreflective tape

Self-mixing interference was observed to arise from optical feedback from a retroreflective tape. In this case, the modulation signal was strong enough to be observed directly on the voltage across the diode as well as on the rear diode emission. With our set-up it was not practical to measure these parameters simultaneously, so the rear emission and the voltage were measured during consecutive experiments. In both cases, for increased sensitivity the $2f$ component of the signal was recorded, and the lock-in amplifier phase was set so as to minimise the background (dc) voltage signal. To ensure that the voltage signal was not directly caused by the laser current modulation at f, a control experiment was conducted in the absence of external feedback.

Figure 11 shows the correspondence between $2f$ components of the laser voltage and the signal received by the monitor photodiode.

This experiment confirms that, for strong self-mixing interference, we can observe the effect as a small modulation

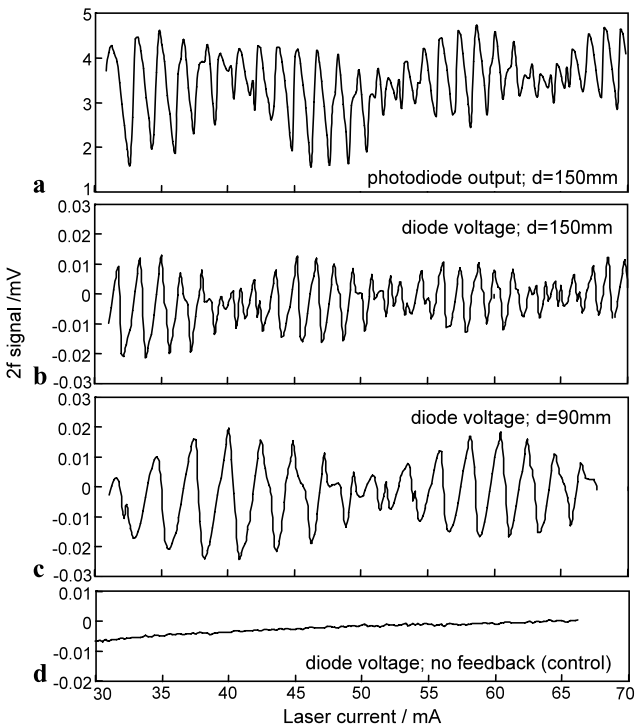

Fig. 11 Comparison of the self-mixing-induced $2f$ signal components (**a**) on the laser monitor photodiode, (**b**), (**c**) on the laser diode voltage, and (**d**) on the laser diode voltage in a control experiment with no external feedback

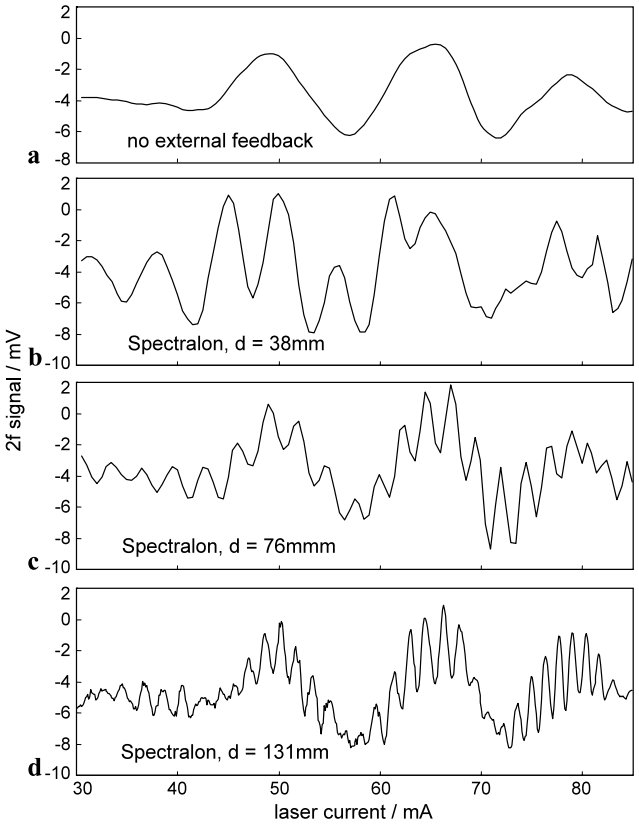

Fig. 12 Self-mixing modulation of the output from the rear facing DFB monitor photodiode by feedback from a Spectralon™ plate placed at different distances from the laser. (**a**) No external feedback, (**b**) $d = 38$ mm, (**c**) $d = 76$ mm, (**d**) $d = 131$ mm

of the laser diode voltage while ramping the drive current. The voltage modulation showed good correspondence with the modulated output intensity and increased its pitch with decreasing cavity length, as expected.

As can be seen from Fig. 11(d), the low signal-to-noise ratios for voltage measurements meant that we were unable to observe the weak spectral feature resulting from feedback within our laser package, as mentioned in Sect. 4.1. The broad fringe envelope observed in Fig. 11(a)–(c) is therefore believed to be associated with the external feedback cavity, and its FSR was observed to change with the cavity length. We have observed this effect repeatably in other experiments involving higher levels of feedback (see Sect. 4.5) but have been unable to determine its precise cause.

4.4 DFB laser with feedback from a diffuse reflector

We recorded self-mixing interference signals using the DFB monitor photodiode, for case of feedback from a diffuse reflector (Spectralon™) placed in the output beam at a range of distances from the laser diode. A sample of the results is shown in Fig. 12. The modulation observed in the absence of external feedback is consistent with the findings of Sect. 4.1.

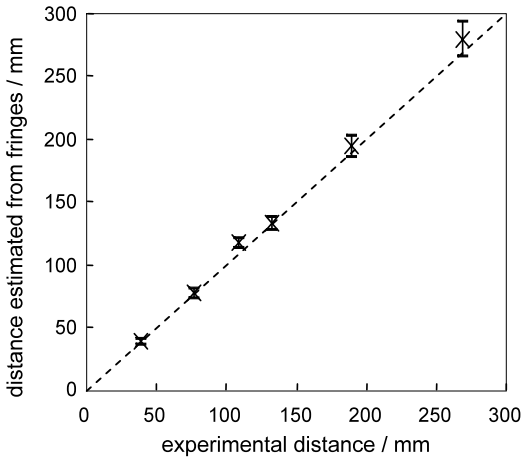

Fig. 13 Results of self-mixing feedback from a diffuse reflector: distance estimated from the fringe count versus measured experimental distance from reflector to laser diode

Further experiments were conducted for d values covering the range 38–268 mm. For each recorded spectrum, we determined the fringe spacing by counting fringes over a defined spectral region and calculated the relevant cavity length using the laser diode current tuning coefficient. The results are shown in Fig. 13.

At a distance of 108 mm, the mean fringe depth was estimated to be equivalent to a gas measurement uncertainty of approximately 400 ppm. At this distance, the proportion of light backscattered by a perfect Lambertian diffuser into a 4.9-mm diameter aperture is estimated using (6) to be $r \approx 8 \times 10^{-4}$. Comparing this result with the equivalent estimate ($r = 0.4\%$) of Sect. 4.2, a reduction in the feedback level by a factor of 5 has resulted in an improvement in the detection uncertainty by a factor of approximately $\sqrt{5}$, in line with the predictions of (5).

4.5 VCSEL with feedback from a retroreflective tape

Confirmation of self-mixing modulation of the output from a VCSEL was hampered by the lack of a rear facet for this laser design. Instead of monitoring the rear emission, we repeated our experiment with retroreflective tape to increase the signal level and monitored the voltage across the diode. Figure 14 shows the results.

These results confirm self-mixing interference behaviour in our VCSEL. The change in fringe spacing with cavity length is again consistent with (5). Again, at these higher levels of feedback, we observed a broad envelope for the narrower fringes, and this envelope appeared to change with the external feedback cavity spacing.

4.6 Gas absorption measurements

A series of gas absorption measurements was made with relatively high levels of self-mixing feedback. In order to

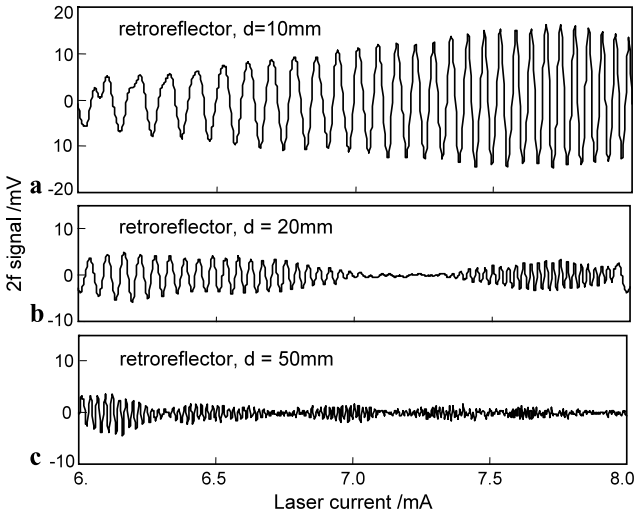

Fig. 14 Self-mixing interference observed as a modulation of the voltage across a VCSEL. Second harmonic signals obtained with retroreflective tape placed at distance d of (**a**) 10 mm, (**b**) 20 mm and (**c**) 50 mm

separate the effects of feedback from possible etalon effects within the gas cell, the configuration in Fig. 15 was used, which is similar to the configuration in Fig. 8. Self-mixing induced interference was confirmed for this configuration using the DFB monitor photodiode, but to combine this with a measurement using a gas cell, we recorded the effects on the forward emission. A pellicle beamsplitter (Thorlabs BP245B3, 45:55 splitting ratio) was used to pass a proportion of the main beam emitted by the DFB laser diode towards a reference detector (D1). The main beam was then directed towards a 6° wedged window, whose front surface was aligned to direct the reflected beam back towards the laser with a reflectivity of approximately 0.4%, the feedback at the laser diode being reduced to 0.1% of the initial intensity after traversing the beamsplitter twice. A conventional gas cell was used with a 10-cm pathlength and 6° wedged AR-coated windows to reduce etalon effects to an insignificant level compared with self-mixing feedback. Transmission through the cell was monitored with a second detector (D2). Signals from both detectors (Thorlabs PDA400) were demodulated at $2f$ using lock-in amplifiers as previously described. With hydrocarbon free air in the gas cell, the $2f$ output from each detector/lock-in amplifier combination was normalised so as to balance the two readings.

In a first experiment, the laser drive current was ramped over the range 30–80 mA in steps of 0.2 mA, while $2f$-demodulated outputs were recorded simultaneously for channels D1 and D2. Scans were taken with different concentrations of methane in air within the gas cell (all at atmospheric pressure). The results are shown in Fig. 16(a) and show self-mixing feedback on both detectors D1 and D2, with a fringe spacing dictated by the distance from the wedged window to the laser diode (64 mm).

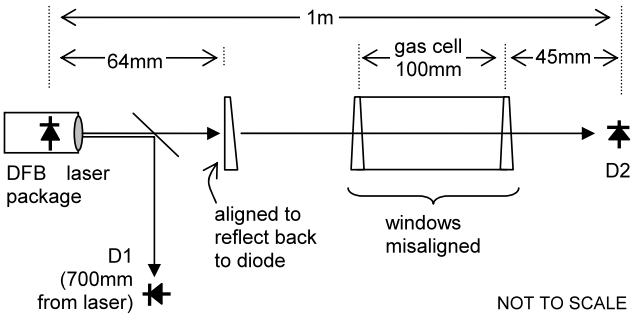

Fig. 15 Configuration of experiments to investigate self-mixing feedback in gas absorption measurements

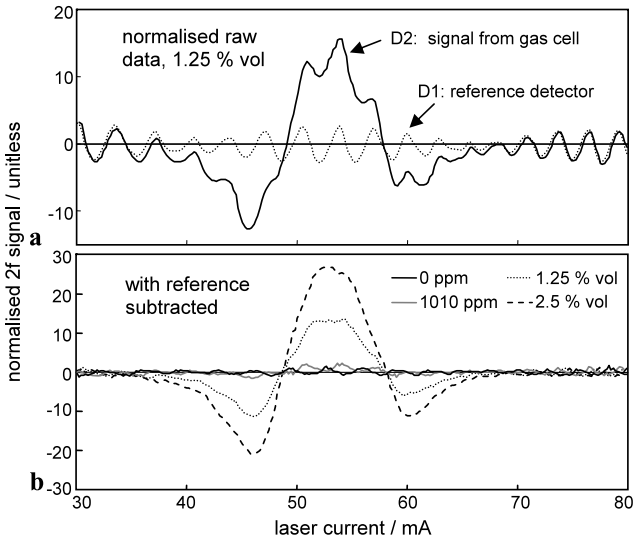

Fig. 16 Results of wavelength scans through a methane line at different concentrations, while high levels of feedback were deliberately applied to the laser diode. (**a**) Normalised $2f$ signal components, (**b**) signals from D2 corrected by subtraction of the reference signal from D1. (Lock-in τ 100 ms)

The fact that self-mixing feedback induces a modulation on the entire laser diode output allows for a straightforward reduction scheme. Here, we have simply subtracted the normalised output from the reference channel D1 (after lock-in demodulation) from that of our main signal channel D2. Figure 16(b) shows that this has removed the modulation to first order. A small residual modulation remains, caused by a slight phase change in δ observed between the two sets of fringes, the precise cause of which is uncertain, but it may be associated with an imbalance in the two photodetector/amplifiers. At 1010 ppm, the methane line is just discernible.

In a second experiment, the laser diode output was locked to the methane line, and $2f$-demodulated outputs from both detectors were recorded simultaneously. Different methane concentrations were delivered to the cell; first hydrocarbon free air, then 1010-ppm methane in air. The results are shown in Fig. 17. Here, subtraction of the demodulated ref-

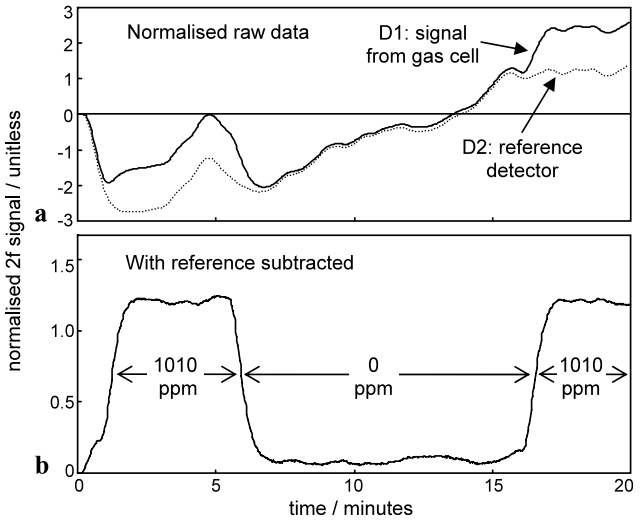

Fig. 17 Normalised $2f$-demodulated output from detectors D1 and D2 plotted as a time series while different methane concentrations (in air) were delivered to the gas cell. (**a**) Normalised raw data, (**b**) data corrected by subtraction of the reference. (Lock-in τ 10 s)

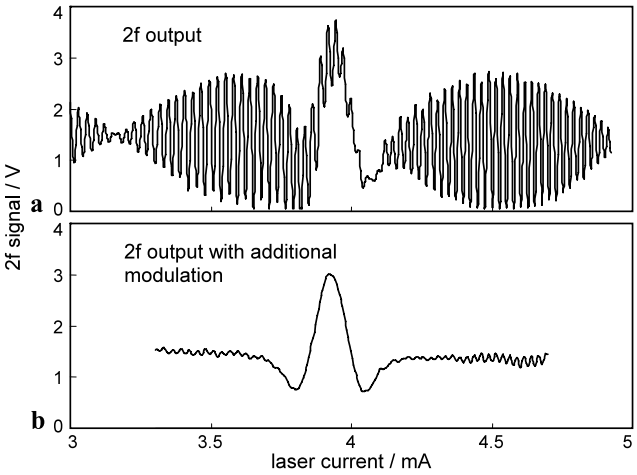

Fig. 18 $2f$ WMS signals acquired by the microLGD™ for a methane concentration of 100 ppm. (**a**) Interference fringes superimposed on the absorption line for straightforward WMS at $f = 20$ kHz. (**b**) Suppression of fringes using an additional low-amplitude modulation

erence signal has improved the signal-to-noise ratio by over a factor of 10, giving an estimated limit of detection of approximately 100 ppm. Residual noise and drift in the corrected signal is attributed to imbalances between the two light paths leading to D1 and D2, possibly caused by etalon effects.

Previous work using balanced detection schemes has been reported, showing a performance improvement when interference fringes are present [14]. Such schemes are similar in principle to the work shown here but have the advantage of closer matching of the measurement and reference channels. However, the nature and source of the fringes has not, to our knowledge, been explicitly reported. Here we show that an "upstream" reference measurement can compensate for the "downstream" generation of fringes.

5 Results for a commercial VCSEL-based instrument

We conducted experiments using a commercial gas detector (IR Microsystems microLGD™). The instrument employs a 1651-nm VCSEL (Vertilas VL-1651-1-SP-T5) mounted in a cell of 80-mm physical length with a reflective geometry and a total path length of 160 mm. The cell has been carefully designed so as to minimise the opportunity for etalons to arise in the optical path, by tilting the photodiode to prevent direct specular reflection from the detector or its package to be redirected towards the laser. A custom electronics board performed laser current and temperature control as well as second harmonic demodulation for WMS. Signals were transferred to a computer running Labview™ software via an RS232 port. The VCSEL was modulated at a frequency $f = \sim$20 kHz to generate a WMS gas detection signal.

Because the instrument configuration was fixed, we were unable to confirm self-mixing interference behaviour directly by any of the techniques used in our laboratory experiments. Instead, we simply recorded $2f$ signals from the photodiode. Figure 18 shows the results of a wavelength scan for a methane concentration of 100 ppm within the cell. For straightforward WMS, a large fringe-like modulation can be observed superimposed on the gas line (Fig. 18(a)). These fringes can be efficiently reduced by applying a mechanical modulation [15] or a deliberate low-amplitude modulation to the laser [16]. Here, suppression of over a factor of 10 has been achieved using the latter technique at 1.6 kHz (Fig. 18(b)).

The fringe spacing was found to correspond to a 16-cm cavity, twice the physical length of the gas cell. Angling or misaligning either the laser or the photodiode did not significantly reduce the fringe visibility. This is consistent with two possible causes, (i) self mixing interference, possibly caused by a small fraction of the light reflected by the mirror falling directly onto the laser diode, and (ii) a weak etalon in the optical path, formed between the photodiode and mirror or the laser diode and mirror. We were unable to confirm unambiguously which of these causes was responsible.

Following suppression of the fringes, the short-term rms noise was established to be approximately 1.8 ppm over a period of 3 minutes, with a longer term zero drift of approximately 10 ppm.

6 Discussion and conclusions

In WMS, the impact of interference fringes caused by etalons in the optical path of gas cells is well known, but to our knowledge, the effects of self-mixing interference have not been explicitly reported. We have shown that the amplitude of the resulting modulation in the laser output can be significant, corresponding to a gas signal at the 900-ppm level for the reflection from an AR-coated wedged window at a distance of 154 mm, or 400 ppm from Spectralon™ at a distance of 108 mm. With our DFB laser diode, we estimate that feedback would have to be reduced to below 1 part in 10^8 to permit detection of methane at 1 ppm within a 100-mm pathlength.

Our experiments used exaggerated levels of optical feedback in order to investigate the effect; in practice we expect that good optical design would reduce this to give decreased fringe amplitudes. As mentioned above, to maximise self-mixing interference signals for the purpose of distance sensing, a large diode collimating/collection lens is often used. Therefore in gas sensing applications (where we wish to minimise the effect) our DFB package design is less than ideal. Better immunity to weak feedback would result from the use of a smaller lens aperture or from reducing the coupling efficiency. This is the case for our VCSEL design, which uses no lens and so has a divergent beam with a divergence angle of $>10°$, and a much smaller entrance aperture for back-reflected light. We indeed observed that the VCSEL was less sensitive to feedback, with good signal-to-noise ratios only achievable for short laser–reflector distances. However, without quantifying the level of returned light to the VCSEL in these experiments, it is difficult to compare the two types of diode directly. Giuliani et al. have compared the sensitivity of different types of laser diode and show that some DFB lasers are more sensitive to feedback than VCSELs, whereas others are less sensitive, depending on the exact design [4].

However we optimise the laser package design; the problem remains that if we want to use the laser diode emission, a return path will remain for feedback. A good quality (60 dB) optical isolator would circumvent the problem by reducing feedback, but for reasons of cost and simplicity, many workers prefer to avoid them, especially for industrial systems. It has indeed been our experience that in small quantities, isolators designed for use at nonstandard wavelengths can cost more than the laser diodes themselves. Furthermore, the problem remains of feedback arising from reflections from the front face of the isolator. However, intensity referencing, as implemented in balanced detection schemes [14], can remove the effects of the modulation to first order. In our simple experiments, referencing improved the signal-to-noise ratio by over a factor of 10.

We have shown that self-mixing interference can arise from specular reflections, but perhaps more importantly from diffuse reflections (in our case, from Spectralon™ and a retroreflective tape). This result means that the presence of dust or dirt within the optical path will also present a problem and could be an issue for gas detectors designed for use in industrial environments. Air filters can be used to protect the optics, but these compromise response times and can themselves become blocked by dirt.

Thus, self-mixing interference fringes can arise in a greater range of circumstances than etalon-induced fringes. Furthermore, if etalons are created by gas cell windows, as is often the case, the two surfaces comprising the etalon have similar, low reflectivities, and the resulting fringes have a modulation depth proportional to r. However, for self-mixing interference, the modulation depth is proportional to $\sqrt{r}$. Therefore, as the value of r reduces, limited in practice by the quality of AR coatings, self-mixing interference is increasingly dominant.

To conclude, we have shown that self-mixing interference can cause spurious signals to arise in gas detectors based on wavelength modulation spectroscopy. As with etalon-induced fringes, the problem is particularly severe for this form of gas detection, which is highly sensitive to curved or periodic spectral features with a free spectral range of the order of the gas absorption linewidth. For methane, this corresponds to an optical path difference of approximately 30 mm. In the very weak feedback regime, the effect is a sinusoidal modulation of the laser diode output, whose amplitude is proportional to the square root of the level of reflected or backscattered light reaching the laser diode. The modulation can be observed on the forward and rear diode emission (for lasers with a rear facet) as well as, for strong signals, on the voltage across the diode.

Acknowledgements This work was carried out under an EPSRC research grant (GR/T04601/01). Jane Hodgkinson is supported by an EPSRC Advanced Research Fellowship (GR/T04595/01).

References

1. H.I. Schiff, G.I. Mackay, J. Bechara, in *Air Monitoring by Spectroscopic Techniques*, ed. by M.W. Sigrist (Wiley, New York, 1994), Chap. 5
2. D.S. Bomse, A.C. Stanton, J.A. Silver, Appl. Opt. **31**(6), 718–730 (1992)
3. J. Hodgkinson, R.D. Pride, C. Tandy, D.G. Moodie, G. Stewart, in *Applications of Optical Fiber Sensors*, ed. by A.J. Rogers. Proc. SPIE, vol. 4074, pp. 90–98 (2000)
4. G. Giuliani, M. Norgia, S. Donati, T. Bosch, J. Opt. A, Pure Appl. Opt. **4**, S283–294 (2002)
5. J. Zhou, M. Wang, D. Han, Opt. Express **14**(12), 5301–5306 (2006)
6. F. Vogel, B. Toulouse, IEEE T. Instrum. Meas. **54**(1), 428–431 (2005)
7. G. Giuliani, S. Bozzi-Pietra, S. Donati, Meas. Sci. Technol. **14**(1), 24–32 (2003)
8. L.S. Rothman et al., J. Quant. Spectrosc. Radiat. Transf. **96**, 139–204 (2005)

9. J.L. Santos, A.P. Leite, D.A. Jackson, Appl. Opt. **31**(34), 7361–7366 (1992)
10. A.E. Ennos, in *Laser Speckle and Related Phenomena*, ed. by J.C. Dainty (Springer, Berlin, 1975), Chap. 6
11. D. Masiyano, J. Hodgkinson, R.P. Tatam, Appl. Phys. B **90**, 279–288 (2008)
12. R.S. Sirohi, Contemp. Phys. **43**(3), 161–180 (2002)
13. T. Igushi, J. Opt. Soc. Am. B **3**(3), 419–423 (1986)
14. L. Persson, F. Andersson, M. Andersson, S. Svanberg, Approach to optical interference fringes reduction in diode laser absorption spectroscopy. Appl. Phys. B **87**, 523–530 (2007)
15. J.A. Silver, A.C. Stanton, Appl. Opt. **27**, 1914–1916 (1988)
16. R. Reid, M. El-Sherbiny, B.K. Garside, E.A. Ballik, Appl. Opt. **19**, 3349–3354 (1980)